

広島大学学術情報リポジトリ  
Hiroshima University Institutional Repository

Title	“Open-Loop” Tracking Interferometer Measurement Using Rotary Axes of a Five-Axis Machine Tool
Author(s)	Ibaraki, Soichi; Tsuboi, Keisuke
Citation	IEEE/ASME Transactions on Mechatronics , 22 (5) : 2342 - 2350
Issue Date	2017-09-04
DOI	<a href="https://doi.org/10.1109/TMECH.2017.2749142">10.1109/TMECH.2017.2749142</a>
Self DOI	
URL	<a href="https://ir.lib.hiroshima-u.ac.jp/00048862">https://ir.lib.hiroshima-u.ac.jp/00048862</a>
Right	© 2017 IEEE. Personal use of this material is permitted. Permission from IEEE must be obtained for all other uses, in any current or future media, including reprinting/republishing this material for advertising or promotional purposes, creating new collective works, for resale or redistribution to servers or lists, or reuse of any copyrighted component of this work in other works. This is not the published version. Please cite only the published version. この論文は出版社版ではありません。引用の際には出版社版をご確認、ご利用ください。
Relation	



# “Open-loop” tracking interferometer measurement using rotary axes of a five-axis machine tool

Soichi Ibaraki and Keisuke Tsuboi

**Abstract**—The tracking interferometer, or the laser tracker, is a laser interferometer with a steering mechanism to change the laser beam direction to automatically follow a retroreflector. Many researchers have studied its application to the multilateration to measure the retroreflector’s three-dimensional position. This paper shows that the multilateration measurement can be done by regulating the laser beam toward the command retroreflector position, assuming that the machine tool’s positioning error is reasonably small. The machine’s rotary axes are used to regulate the laser beam direction. The proposed scheme enables a user to perform the multilateration measurement by using a laser interferometer and the machine’s rotary axes only, without requiring any specialized tracking mechanism. An experiment is presented to investigate its measurement performance. The paper’s emphasis is on the assessment of its measurement uncertainty, introduced by the elimination of automated tracking mechanism.

## I. INTRODUCTION

THE term “volumetric accuracy” of a machine tool is defined in ISO 230-1 [1] revised in 2012. A Technical Report (TR) on numerical compensation for machine tool volumetric errors is now available in ISO/TR 16907 [2]. Such efforts indicate that more machine tool manufacturers and users recognize the importance of evaluating the volumetric accuracy of a machine tool. Many latest commercial CNC systems have the functionality of numerically compensating for volumetric errors.

Suppose that the command tool center position (TCP) is given by  $p^* \in \mathbb{R}^3$  in the machine coordinate system. Denote its actual position by  $p \in \mathbb{R}^3$ . The three-dimensional (3D) positioning error,  $\Delta p \in \mathbb{R}^3$ , is defined by  $\Delta p(p^*) \equiv p - p^*$ . The assessment of a machine tool’s volumetric accuracy requires the measurement of  $\Delta p(p^*)$  at arbitrary  $p^*$  in the machine’s workspace.

This is a difficult metrological problem. The volumetric accuracy is typically assessed through the measurement of each geometric error of individual axis (“indirect measurement”). The references [3], [4] present a good review of conventional indirect volumetric accuracy measurement schemes. A tracking interferometer (the term in [1]), or the laser tracker, is recognized as only commercially available instrument capable of directly measuring the 3D TCP position at an *arbitrary* location within its workspace. It is a laser interferometer with

a steering mechanism to change the laser beam direction to automatically follow a retroreflector. Lau et al. first reported this instrument in the mid-1980s [5]. In today’s market, many commercial products are available with a wide range of industrial applications, as reviewed in [6]. Many commercial tracking interferometers measure the retroreflector’s position from the distance to it and the direction of the laser beam. Since its angular measurement uncertainty directly contributes to the measurement uncertainty, it is typically difficult to ensure the measurement accuracy high enough to evaluate machine tools.

On the other hand, the multilateration measurement (the term in [1]) estimates the retroreflector’s 3D position by the distances from typically four or more tracking interferometers (see Fig. 1). Since it does not use the angular orientation of the laser beam in its calculation, its measurement uncertainty is typically lower. Its application to the error calibration of a machine tool or a coordinate measuring machine (CMM) has been long studied [7], [8], [9]. Its commercial product is available (Etalon [10], [11]).

When a machine tool is measured, the retroreflector’s command position in the machine coordinate system is given. The distance from the laser interferometer to the retroreflector can be measured by regulating the laser beam toward the command retroreflector position. The machine’s positioning error only imposes the “cosine error” on the laser length. When it is sufficiently small, the multilateration measurement can be done without the automated tracking mechanism, i.e. a photodiode and a feedback control system for laser beam direction. In Refs. [12] (2D version) and [13] (3D version), a part of the authors referred this concept to as the “open-loop” tracking interferometer and presented its prototype.

In our previous works [12], [13], the prototype “open-loop” tracking interferometer had two numerically-controlled rotary drives to regulate the laser beam direction to the given command position of the retroreflector. By further extending this concept, this paper presents the implementation of the “open-loop” tracking interferometer by using rotary axes of a five-axis machine tool. When the machine tool has two rotary axes, the multilateration measurement can be performed by using a laser interferometer only, requiring any other specialized instrument. This lower-cost implementation of the multilateration measurement is a major practical contribution of this paper. We claim that this could significantly widen the multilateration measurement’s application in the machine tool industry. For example, potentially, the present multilateration measurement can be performed by a machine tool builder along with a conventional linear positioning error test using a laser interferometer, without requiring an expensive

S. Ibaraki (corresponding author) was with Department of Mechanical Systems Engineering, Hiroshima University, Kagamiyama 1-4-1, Higashi Hiroshima, Hiroshima 739-8527, Japan, e-mail: ibaraki@hiroshima-u.ac.jp.

K. Tsuboi was with the Department of Micro Engineering, Kyoto University, Katsura, Nishigyo-ku, Kyoto 615-8530, Japan.

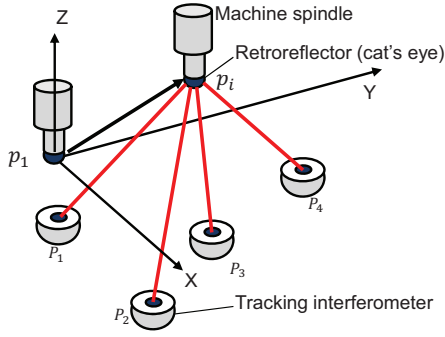


Fig. 1. Multilateration measurement setup [9].

tracking interferometer. To investigate the validity of the present scheme compared to conventional automated tracking interferometers, the paper's emphasis will be on the evaluation of its measurement uncertainty introduced by the elimination of automated tracking mechanism.

## II. PROPOSED MEASUREMENT SCHEME

### A. Review: conventional tracking interferometer and multilateration algorithm

A conventional "automated" tracking interferometer has a mechanism to regulate the laser beam direction to follow the retroreflector. Its typical mechanism is illustrated in Fig. 2. The laser beam direction is controlled so that the laser spot position on the quadrant photo-diode is regulated at the reference point.

Suppose that the retroreflector is positioned at the  $i$ -th command position,  $p_i^* \in \mathbb{R}^3$  ( $j = 1, \dots, N$ ). The tracking interferometer's rotation center is located at  $P_j^* \in \mathbb{R}^3$  ( $j = 1, \dots, N_j$ ) (see Fig. 1). The objective of the multilateration measurement is to estimate the retroreflector position,  $p_i \in \mathbb{R}^3$ , from the laser displacement,  $\Delta L_{ij} \in \mathbb{R}$ . This problem differs from the classical trilateration in that 1) the exact position of each tracking interferometer is not known, and 2) only the relative distance from the initial position can be measured by a laser interferometer. A self-calibration approach to solve this problem has been well developed [10], [9]. This subsection only briefly reviews it.

The problem can be written as the following minimization problem:

$$\min_x \sum_{i=1 \dots N_i, j=1 \dots N_j} (f_{ij}(x) - \Delta L_{ij})^2 \quad (1)$$

where:

$$f_{ij}(x) = \|p_i - P_j\| - L_{0j} \quad (2)$$

$L_{0j} \in \mathbb{R}$  represents the dead path length in the measurement by the  $j$ -th tracking interferometer [10].  $x \in \mathbb{R}^{3N_i + 4N_j}$  represents a set of unknown parameters to be identified, containing:

$$x = \left[ \{p_i\}_{i=1, \dots, N_i}, \{P_j\}_{j=1, \dots, N_j}, \{L_{0j}\}_{j=1, \dots, N_j} \right] \quad (3)$$

The coordinate system can be set up arbitrarily, and total six parameters in  $x$  can be constrained according to the coordinate system setup (see [9]). For  $3N_i + 4N_j - 6$

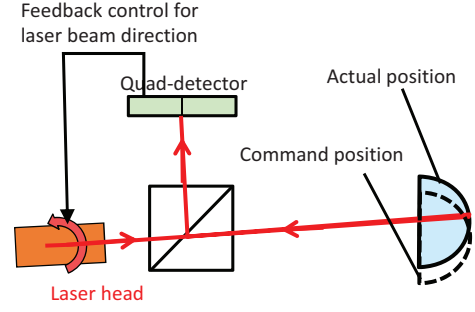


Fig. 2. Typical tracking mechanism in conventional "automated" tracking interferometer [13].

unknown parameters, the number of laser measurements is  $N_i \cdot N_j$ . Therefore, when  $N_i > \frac{4N_j - 6}{N_j - 3}$ , the number of measurements exceeds the number of unknown parameters. Define  $f := \{f_{ij}\}_{i=1 \dots N_i, j=1 \dots N_j} : \mathbb{R}^{3N_i + 4N_j} \rightarrow \mathbb{R}^{N_i \cdot N_j}$  and  $\Delta L := \{\Delta L_{ij}\}_{i=1 \dots N_i, j=1 \dots N_j} \in \mathbb{R}^{N_i \cdot N_j}$ . An iterative linearization-based approach is typically used to locally solve the problem (1):

$$\hat{x}^{(k+1)} = \hat{x}^{(k)} + \left( A^{(k)T} A^{(k)} \right)^{-1} A^{(k)T} \left( \Delta L - f(\hat{x}^{(k)}) \right) \quad (4)$$

where

$$A^{(k)} := \left. \frac{\partial f}{\partial x} \right|_{x=\hat{x}^{(k)}} \quad (5)$$

### B. Proposed scheme: principle

As is illustrated in Fig. 3, the instrument's angular positioning error only impose the "cosine error" on the laser displacement. In the multilateration principle, therefore, the laser beam's orientation error does not impose significant contribution on the measurement uncertainty. In the application to machine tool calibration, the retroreflector's command position in the machine coordinate system is given. It is, furthermore, reasonable to assume that the machine's positioning error is sufficiently small to make its "cosine error" negligibly small. In such a condition, the multilateration measurement can be done by regulating the laser beam toward the command retroreflector position, requiring no automated tracking mechanism. In this paper, this scheme is called the "open-loop" tracking interferometer; "open-loop" in the sense that the retroreflector's actual position is not fed back to the control of laser beam direction (unlike the automated tracking in Fig. 2). It must be emphasized that the paper does not assume that the machine's positioning error is negligibly small. The machine's positioning error is assumed to be smaller than some certain level, such that this "cosine error" in laser lengths is negligibly small. Section IV will present the uncertainty analysis to show that this influence is not significant on "typical" commercial machine tools.

This paper considers a five-axis machine tool with two rotary axes in the tool side shown in Fig. 4 a). Its axis designation [14] is [w X' b Z Y C A (C) t]. A laser interferometer is attached on the spindle's face plate such that the laser beam is approximately on the spindle axis of

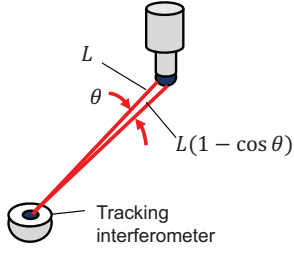


Fig. 3. The influence of the orientation error of the laser beam on the laser displacement (“cosine error”) [12].

rotation. A retroreflector is attached to the work table. A cat’s eye retroreflector is typically used. A cat’s eye retroreflector is a spherical glass of sufficiently high geometric accuracy with its hemispheric surface coated by the total-reflection metal-film deposition [15].

The following assumptions are made:

- 1) In the machine coordinate system, the retroreflector’s center position,  $P_j^* \in \mathbb{R}^3$  ( $j = 1, \dots, N_j$ ), is roughly known.
- 2) When  $A = 0^\circ$ , the laser beam is approximately parallel to the machine’s Z-axis. When  $C = 0^\circ$  and  $A = 90^\circ$ , the laser beam is approximately parallel to the machine’s Y-axis.

The nominal intersection of A- to C-axis centerline is referred to as *the spindle’s reference point* in this paper. Its  $i$ -th command position,  $p_i^* \in \mathbb{R}^3$  ( $i = 1, \dots, N_i$ ), is given in the machine coordinate system. The origin of the machine coordinate system is set at an arbitrary position in the workspace. Then, the laser beam is directed to the  $j$ -th retroreflector’s center,  $P_j^*$ , by regulating A- and C-axis angular positions as follows:

$$\begin{aligned} a_{ij}^* &= \cos^{-1} \left( \frac{P_j^*(3) - p_i^*(3)}{\|P_j^* - p_i^*\|} \right) \\ c_{ij}^* &= \tan^{-1} \left( -\frac{P_j^*(1) - p_i^*(1)}{P_j^*(2) - p_i^*(2)} \right) \end{aligned} \quad (6)$$

Figure 4 illustrates the proposed measurement scheme. When the spindle’s reference point is commanded at an arbitrary (X, Y, Z) position, A- and C-axes are regulated such that the laser beam is oriented to the retroreflector. When the retroreflector is fixed at  $P_j^*$ , a set of the spindle’s command positions,  $p_i^*$  ( $i = 1, \dots, N_i$ ), is measured. To perform the multilateration measurement shown in Fig. 1, the laser displacement must be measured from at least four different retroreflector positions,  $P_j^*$  ( $j = 1, \dots, N_j$ ).

### C. Initial estimation of zero angular positions and retroreflector position

The following procedure is performed to meet the assumptions 1) and 2) in Section II-B:

#### (1) Adjustment of zero angular position of rotary axes

At  $C = 0^\circ$ , the A-axis zero angular position is set so that the laser beam is aligned parallel to the machine’s Z-axis reference

straight line. This alignment can be done by searching for the A-axis angular position to minimize the measured laser displacement, when the retroreflector is moved to the Y- or X-direction by a small distance (see Fig. 5). Similarly, at  $A = 90^\circ$ , the C-axis zero angular position is searched so that the laser beam is aligned parallel to the machine’s Y-axis reference straight line.

#### (2) Initial estimation of retroreflector position

The 3D position of the retroreflector in the machine coordinate system is estimated as follows: position the spindle’s reference point at each vertex of the workspace. Denote this command position in the machine coordinate system by  $p_i^* \in \mathbb{R}^3$  ( $i = 1, \dots, N_i$ ). Then, manually find the A- and C-axis angular positions, denoted by  $a_i, c_i \in \mathbb{R}$ , where the laser beam is reflected by the retroreflector and reaches the detector (see Fig. 6). The unit direction vector to represent the laser beam direction is given by:

$$v_i = \begin{bmatrix} -\sin a_i \cos c_i & \sin a_i \cos c_i & -\cos c_i \end{bmatrix} \quad (7)$$

The retroreflector’s position,  $P \in \mathbb{R}^3$ , can be estimated by solving the following minimization problem:

$$\begin{aligned} \min_P \sum_{i=1}^{N_i} \|e_i\| \\ e_i &:= p_i^* - P + t_i \cdot v_i \\ t_i &:= v_i \cdot (P - p_i^*) \end{aligned} \quad (8)$$

Notice that  $\|e_i\|$  represents the distance from  $P$  to the line representing the laser beam.

Clearly, there are many potential uncertainties in (1) and (2): a) Rotary axis location errors. For example, when there exists the squareness error between the A- and Z-axis average lines, it may not be possible to perfectly align the laser beam to the Z-axis, no matter how the A-axis angular position is adjusted. b) The machine’s actual position always has some error from its command position,  $p_i^*$ . c) The laser beam may not be accurately directed to the center of the retroreflector.

The operations above only give initial estimates needed for the command generation in Eq. (6). Of course, when the error in (1) and (2) is very large, the laser beam would not be directed to the retroreflector’s center by Eq. (6) and the tracking measurement would fail. When it is within a “typical” level, however, its influence would not be significant, since it only gives the “cosine error” on the laser beam length. The influence of the adjustment errors in (1) and (2) on the overall uncertainty will be quantitatively analyzed in Section IV.

### D. Algorithm to estimate retroreflector positions

The algorithm’s objective is to assess error motions of X-, Y-, and Z-axes by calculating actual positions of the spindle’s reference point,  $p_i$  ( $i = 1 \sim N_i$ ). It does not assess error motions of two rotary axes. As will be studied in Section IV, a part of rotary axis location errors, as well as their radial error motions, can be a major uncertainty contributor for the proposed scheme.

For the  $j$ -th retroreflector position, when the spindle’s reference point is positioned at the  $i$ -th command position,

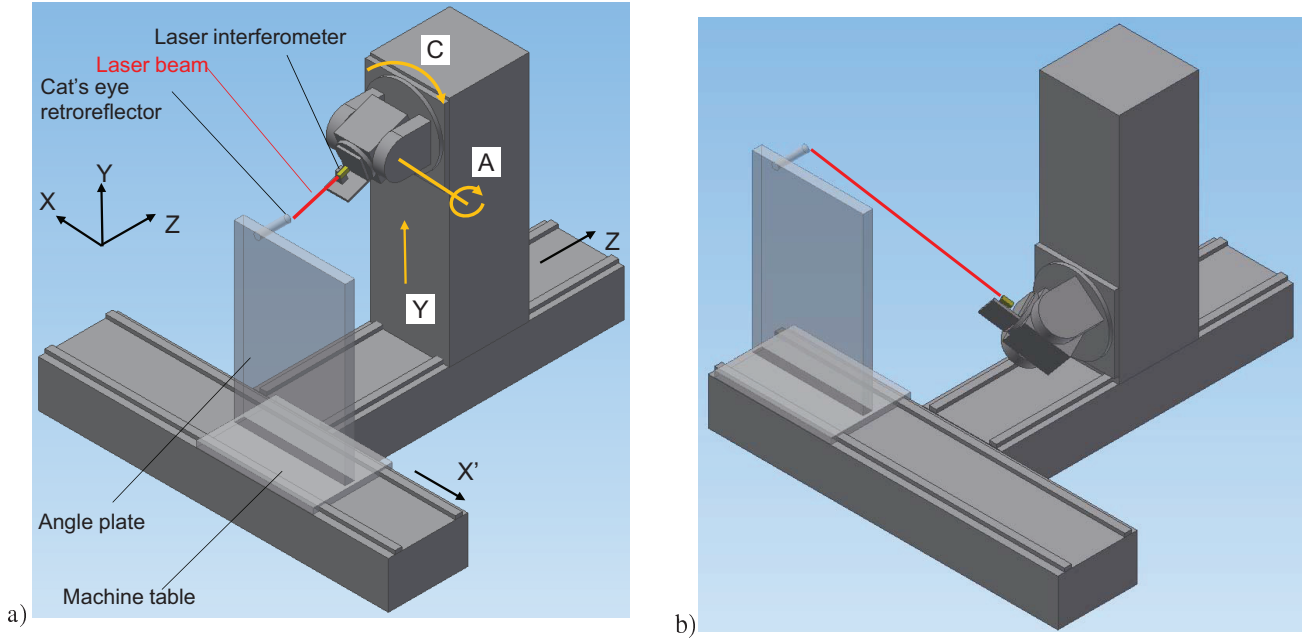


Fig. 4. Proposed tracking operations at various spindle positions. The two rotary axes, A- and C-axes, are regulated such that the laser beam is oriented to the cat's eye retroreflector. a) Machine configuration and test setup. b) Both A- and C-axes are regulated to direct the laser beam to the retroreflector. For each spindle position, at least four laser displacements must be measured for different retroreflector positions (see Fig. 1).

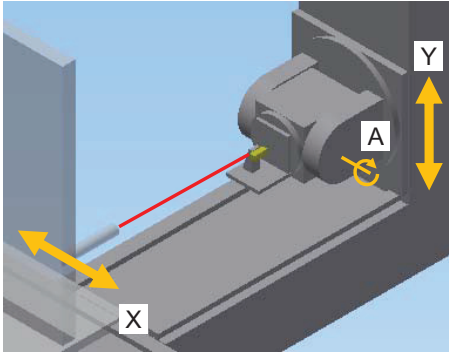


Fig. 5. Adjustment of zero angular position of A-axis. When X- and Y-axes are moved by a small distance, the A-axis angular position is aligned such that the measured laser displacement is minimized.

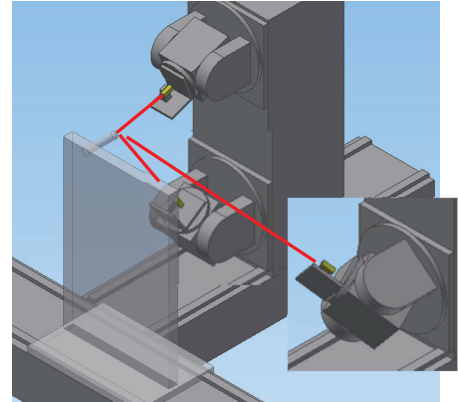


Fig. 6. Initial estimation of retroreflector position. For at least three different machine positions (X, Y, Z), the A- and C-axis angular positions are manually searched such that the laser beam is reflected by the retroreflector and reaches the detector.

$p_i^*$  ( $i = 1 \sim N_i$ ), the laser beam is directed to the direction ( $a_{ij}^*, c_{ij}^*$ ), given in Eq. (6), and the laser displacement,  $\Delta L_{ij} \in \mathbb{R}$ , is measured. This is repeated with different retroreflector positions ( $j = 1 \sim N_j$ ,  $N_j \geq 4$ ). The algorithm to estimate actual positions of spindle's reference point,  $p_i$  ( $i = 1 \sim N_i$ ), is exactly the same as the one reviewed in Section II-A (Eq. (1)).

The original contribution of this paper is on the implementation of the tracking interferometer measurement using the machine tool's rotary axes. The uncertainty analysis to be presented in Section IV will clarify the conditions that the machine tool, the measuring instrument, and the setup must meet, such that the influence of this "open-loop" tracking to the overall uncertainty is sufficiently low.

### III. EXPERIMENT

#### A. Experimental setup

The machine configuration is shown in Fig. 4. A laser interferometer is attached to the machine's spindle face plate by using the fixture shown in Fig. 7. Three screw-driven adjustment stages are used to minutely move the laser interferometer in X- and Y-directions, and to rotate around the Y-axis (notice that the laser beam direction around the X-axis can be adjusted by using the machine's A-axis). The laser beam direction was roughly adjusted to the spindle axis of rotation by using these adjustment stages. Major specifications of the laser interferometer and the cat's eye retroreflector are shown respectively in Tables I and II. Figure 8 shows the experimental

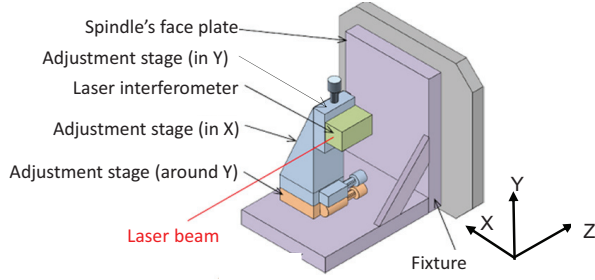


Fig. 7. A fixture to attach a laser interferometer to the machine's spindle face plate.

TABLE I  
MAJOR SPECIFICATIONS OF THE LASER INTERFEROMETER (DISTAX  
L-IH-302A BY TOKYO SEIMITSU CO., LTD.).

Laser	He-Ne laser (vacuum wavelength 633.0 nm)
Measurement range	10 m
Measurement resolution	$\lambda/64 (\approx 0.01\mu\text{m})$
Maximum response speed	$630 \text{ sec}^{-1}$
Measurement uncertainty	$\pm( L  \times 10^{-7} + 0.005 \times 10^{-6}) \text{ m}$ where $L$ is the measurement length.

setup.

Figure 9 shows the retroreflector positions (Positions a to d) and the command trajectory of spindle's reference point. Each retroreflector position was estimated by the procedure in Section II-C(2) as shown in Table III. The spindle's reference point is positioned at total 64 points within  $X800 \times Y800 \times Z800$  mm. At every 100 mm, the machine was stopped for 3 sec and the laser displacement was measured. The command angular positions of A- and C-axes are calculated by Eq. (6) at every 0.1 mm such that the laser beam continuously reaches the retroreflector along the command trajectory.

### B. Experimental result

Figure 10 shows spindle reference positions estimated by solving Eq. (1). An error of the estimate from its command position is magnified 1,000 times ("Error scale"). Figure 11 shows its projection onto (a) the XY plane, and (b) onto the ZX plane.

**Comparison with other direct measurements:** For the comparison, the linear positioning deviation of the Y-axis,  $E_{YY}$ , was directly measured by using a laser interferometer. Figure 12 shows its comparison. The maximum difference between measured and estimated linear positioning deviations was about  $8 \mu\text{m}$  (at  $Y700$  mm) over 800 mm. This difference is within the uncertainty analyzed in Section IV and thus the uncertainty in the proposed scheme can be a major cause for the difference. It is, however, difficult to find a clear cause for this difference. The direct measurement of  $E_{YY}$  by a laser interferometer is also subject to the measurement uncertainty. The direct measurement of  $E_{YY}$  was done a couple of hours after the tracking tests and there can have

TABLE II  
MAJOR SPECIFICATIONS OF THE CAT'S EYE RETROREFLECTOR (BY  
ETALON AG).

Viewing angle	$\pm 80^\circ$
Optical form deviation <sup>1</sup> (circularity)	$< 0.2\mu\text{m}$

<sup>1</sup>: calibrated by the manufacturer.

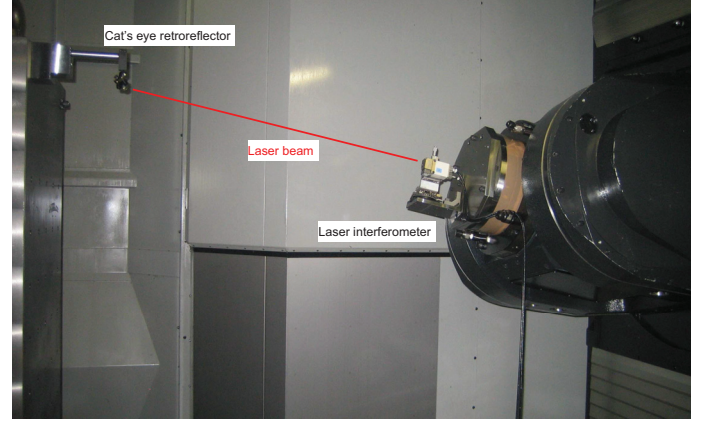


Fig. 8. Experimental setup.

been some change in the machine's volumetric error due to e.g. thermal influence. It should be also noted that the estimates are calculated at  $(X, Z) = (0, -800)$ . On the other hand, the direct measurement by a laser interferometer was done at  $(X, Z) = (394.5, -910.8)$  mm, due to some difficulty in the experiment to put the interferometer at the same position as the estimates. These influences may cause the difference observed in Fig. 12.

For further comparison, squareness errors were measured using a square and a linear displacement sensor, as shown in Table IV. The squareness errors are taken for comparison, since this machine had relatively large squareness errors, as can be observed in Fig. 10. While  $E_{C(0X)Y}$  (the squareness error of Y- to X-axis) and  $E_{C(0Y)Z}$  (Z- to Y-axis) show a good match,  $E_{B(0X)Z}$  (Z- to X-axis) shows larger difference. This is partly because the estimated squareness was calculated from two points in the Z-direction, unlike X- and Y-directions where 10 points were taken (see Fig. 9).

## IV. UNCERTAINTY ANALYSIS

### A. Objective of uncertainty analysis

The proposed "open-loop" tracking procedure has uncertainty contributors that are in principle negligible in conventional automated tracking interferometers. For example, when the machine tool's positioning error is extremely large, the laser beam orientation error to the retroreflector center would naturally increase, which may cause significant "cosine error" (see Fig. 3). In conventional tracking interferometers with an automated tracking mechanism (Fig. 2), this contribution can be negligibly small, when the tracking accuracy is sufficiently high.

To validate the proposed scheme, it is particularly important

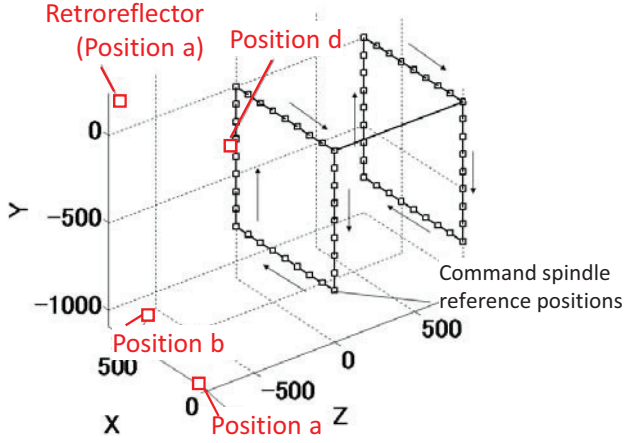


Fig. 9. Command positions of spindle's reference point and the cat's eye retroreflector positions.

TABLE III  
ESTIMATED CAT'S EYE RETROREFLECTOR POSITIONS.

Retroreflector	(X, Y, Z) (mm)
Position a	(80.8, -1093.6, -790.8)
Position b	(731.3, -1071.4, -602.5)
Position c	(67.4, 217.2, -640.3)
Position d	(718.5, 244.3, -792.4)

to show that the uncertainty contributors, existing only in the “open-loop” tracking measurement, do not impose significant influence on the overall measurement uncertainty, when the machine tool, as well as the measuring instrument and its setup, has “typical” accuracy. The present uncertainty analysis is essential to clarify the conditions that the machine tool, the measuring instrument, and the setup must meet. The uncertainty analysis presented in this section is analogous to the ones presented in the authors' previous works [12], [13]. In [12], [13], a specialized measuring instrument was designed to perform the “open-loop” tracking measurement, and its uncertainty was analyzed.

### B. Uncertainty budget for laser displacements

Table V shows the extended uncertainty,  $U(k=2)$ , of the laser displacement when the retroreflector is at Position a, and the spindle reference point is at  $(X, Y, Z)=(0, 0, 800)$  in Fig. 9. The uncertainty significantly depends on their positions. Table V just shows the analysis for a single spindle position as an example to illustrate each contributor's influence. “Type A” uncertainties are assessed by actually measuring the experimental instrument. “Type B” uncertainties are assessed by using the instrument's catalog or specifications.

The following contributors can be in principle negligible in the conventional automated trackers, but inherently exist in the proposed “open-loop” tracking interferometers:

- *Uncertainty in the laser beam direction due to the machine's positioning error from the command position.* ( $u_{414}$ ,  $u_{424}$ ): As discussed in Section IV-A, the uncertainty in the laser beam orientation ( $u_4$ ) can be negligibly

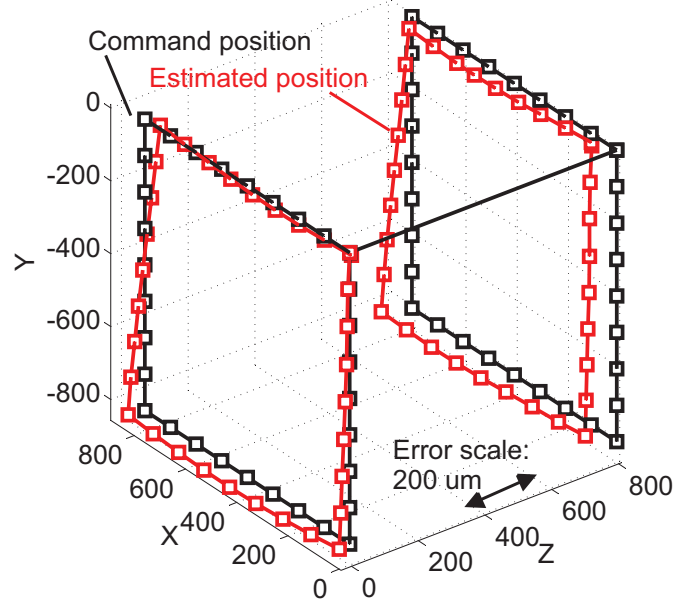


Fig. 10. Estimated spindle reference point positions by the proposed scheme (in 3 view). The error between estimated and command positions is magnified 1,000 times (see “Error scale”).

TABLE IV  
MEASURED AND ESTIMATED SQUARENESS ERRORS.

	X-Y $E_{C(0X)Y}$	Z-Y $E_{A(0Y)Z}$	X-Z $E_{B(0Z)X}$
Direct measurement by using a square	$-40\mu\text{m}$ /800mm	$+3\mu\text{m}$ /800mm	$+59\mu\text{m}$ /800mm
Estimated by the proposed scheme	$-41\mu\text{m}$ /800mm	$+16\mu\text{m}$ /800mm	$+94\mu\text{m}$ /800mm

small in the conventional “automated” tracking interferometer. In the proposed scheme, the laser beam is never directed exactly to the retroreflector's center, since the exact position of the spindle reference point is unknown due to the machine's 3D positioning error. The machine's 3D positioning error is modelled as a normally-distributed random number of the standard deviation assessed based on the estimated volumetric error in Fig. 10. According to  $u_{414}$  and  $u_{424}$  in Table V, its influence on the laser displacement is the “cosine error” and negligible in this setup.

- *Uncertainty in initial estimation of the zero angular position of rotary axes and the retroreflector position.* ( $u_{411}$ ,  $u_{413}$ ,  $u_{421}$ ,  $u_{423}$ ): When the zero angular position of rotary axes, adjusted by the procedure in Section II-C(1), has a significant error, it also causes the laser beam direction error (see Eq. (6)). This error can be caused by the measurement uncertainty in the laser displacement or the squareness error of the machine's linear axes. According to  $u_{411}$  and  $u_{421}$  in Table V, its influence on the laser displacement is also the “cosine error” and is negligibly small. The influence of the error in the retroreflector position, estimated by the procedure



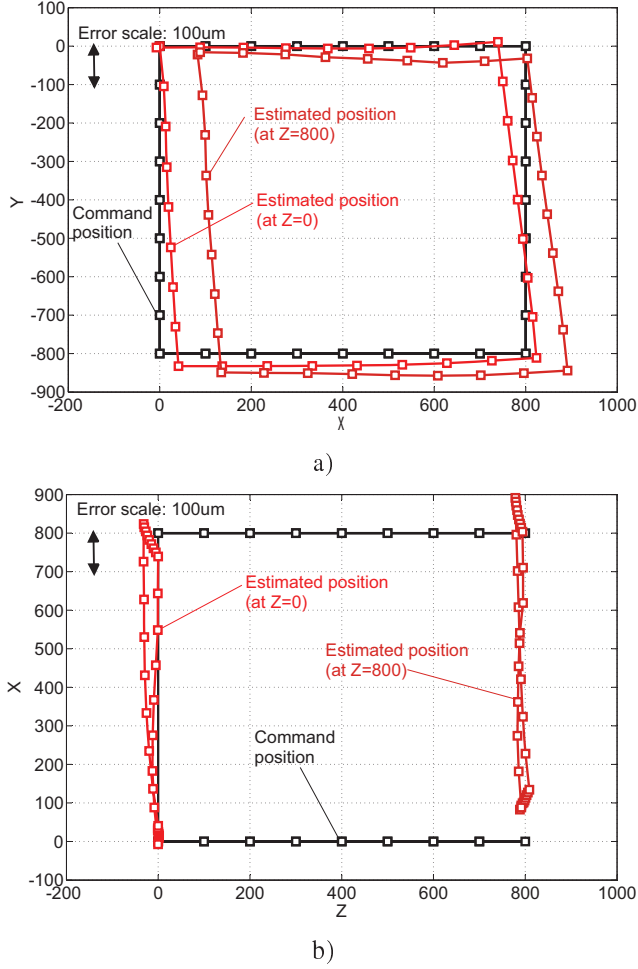


Fig. 11. The projection of Fig. 10 a) onto the XY plane, and b) onto the ZX plane.

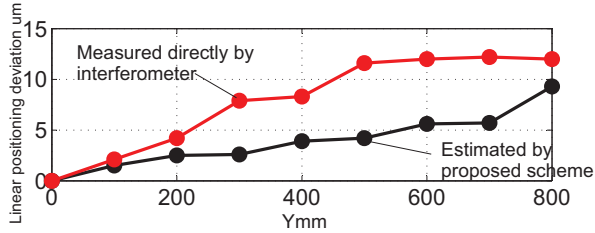


Fig. 12. Comparison of the Y-axis linear positioning deviation,  $E_{YY}$ , measured directly by a laser interferometer and its estimate by the proposed scheme.

in Section II-C(2), can be assessed similarly ( $u_{413}$  and  $u_{423}$ ).

In Table V,  $u_1$  represents the uncertainty in the laser interferometer distance measurement, i.e. the uncertainty in the wavelength ( $u_{11}$  to  $u_{13}$ ), as well as the machine's unrepeatable positioning error ( $u_{14}$ ).  $u_2$  represents the contribution of the interferometer's position error in the direction parallel to the laser beam. Clearly it directly affects the laser beam length. The error motions in the direction normal to the laser beam do not contribute on the laser displacement at all ( $u_3$ ).

*Contribution by error motions of rotary axes:* The radial error motions of the machine's rotary axes directly contribute on  $u_2$ , and therefore the laser displacement. Position and orientation errors of A- and C-axis average lines are parameterized by eight location errors (see [1], [3]). Among them, only the position error of A- to C-axis average line, namely  $E_{Y(OC)A}$ , directly influences the laser displacement. Other location errors, e.g. orientation errors of rotary axis average lines, only influence  $u_4$  and thus its influence on the laser displacement is minor. The experimental machine tool can perform an automated test to calibrate and then numerical compensate for rotary axis location errors by using a touch-triggered probe and a precision sphere (similar automated tests can be done in many latest five-axis machines [3]). Linear axis error motions are one of major uncertainty contributors in such a test. In Table V, linear axis error motions are assessed in the same way as in  $u_{414}$  and  $u_{424}$ , and then its contribution on  $E_{Y(OC)A}$  is assessed in an analogous way as in [19].  $u_2$  is assessed with this influence taken into consideration.

The contributors,  $u_1$ ,  $u_2$ ,  $u_{412}$ ,  $u_{422}$  can be in principle present also in automated tracking interferometers. The measurement uncertainty of conventional "automated" tracking interferometers is extensively studied in [16], [17]. Table V indicates that their contribution is significantly larger. The present analysis validates that the "open-loop" regulation of laser beam direction does not significantly contribute on the uncertainty of the multilateration measurement.

### C. Uncertainty in spindle position estimation

Finally, the uncertainty propagation to estimated spindle positions is calculated by applying the Monte Carlo simulation [18], [19] to the calculation presented in Section II-D. Figure 13 shows the extended uncertainty ( $k = 2$ ) in the estimated spindle positions,  $p_i$  ( $i = 1 \sim N_i$ ) (the distance to the command position).

It must be emphasized that the propagation of the uncertainty in laser displacements to the uncertainty in estimated spindle positions is in principle the same for the conventional "automated" tracking interferometer.

## V. CONCLUSION

Assuming that the machine tool's positioning error is small enough to make its influence on the laser displacement sufficiently small ("cosine error"), the multilateration measurement can be done by regulating the laser beam toward the command retroreflector position. This paper proposed the application of the machine's rotary axes to regulate the laser beam direction. The proposed scheme enables a user to perform the multilateration measurement by using a laser interferometer only, when the machine tool to be measured has two rotary axes.

Unlike conventional "automated" tracking interferometers, the proposed scheme potentially has the following uncertainty contributors. 1) the uncertainty in the laser beam direction due to the machine's positioning error from the command position, and 2) the uncertainty in initial estimation of the zero angular position of rotary axes and the retroreflector position.

TABLE V  
ERROR BUDGET FOR LASER DISPLACEMENT UNCERTAINTY ( $k = 2$ ) AT THE SPINDLE POSITION  $(X, Y) = (100, 100)$  MM AND THE INTERFEROMETER POSITION A.

Symbol	Contributor	Contribution in laser displacement uncertainty	Type
$u_1$	Uncertainty in laser length	$0.65 \mu\text{m}$	
	$u_{11}$ Wavelength accuracy	$0.02 \mu\text{m}$	B
	$u_{12}$ Wavelength correction	$0.14 \mu\text{m}$	B
	$u_{13}$ Environmental change	$0.07 \mu\text{m}$	A
	$u_{14}$ Machine's Repeatability	$0.63 \mu\text{m}$	A
$u_2$	Uncertainty in interferometer position in laser direction	$3.0 \mu\text{m}$	
	$u_{21}$ Radial error motion of A-axis	$2.12 \mu\text{m}$	A
	$u_{22}$ Radial error motion of C-axis	$2.12 \mu\text{m}$	A
$u_3$	Uncertainty in interferometer position error in direction normal to laser	$\approx 0 \mu\text{m}$	
$u_4$	Uncertainty due to laser beam orientation error	$0.54 \mu\text{m}$ (calculated from $u_{41}$ and $u_{42}^\dagger$ )	
$u_{41}$	Uncertainty in laser beam orientation by A-axis	$8.02 \times 10^{-4}$ rad	
	$u_{411}$ Uncertainty in A-axis zero angular position	$0.03 \times 10^{-4}$ rad	B
	$u_{412}$ Angular positioning error of A-axis	$0.18 \times 10^{-4}$ rad	A
	$u_{413}$ Measurement error of retroreflector position	$7.61 \times 10^{-4}$ rad	A
	$u_{414}$ Uncertainty due to machine tool positioning error	$0.40 \times 10^{-4}$ rad	A
$u_{42}$	Uncertainty in laser beam orientation by C-axis	$7.21 \times 10^{-4}$ rad	
	$u_{421}$ Uncertainty in C-axis zero angular position	$0.04 \times 10^{-4}$ rad	B
	$u_{422}$ Angular positioning error of C-axis	$0.18 \times 10^{-4}$ rad	A
	$u_{423}$ Measurement error of retroreflector position	$6.73 \times 10^{-4}$ rad	A
	$u_{424}$ Uncertainty due to machine tool positioning error	$0.34 \times 10^{-4}$ rad	A

†: When the laser beam has directional errors,  $\Delta a_{ij}$  around the X-axis and  $\Delta c_{ij}$  around the Z-axis, the measured laser beam displacement,  $\Delta L_{ij}$ , is influenced by  $L_{ij}^* (1 - \cos \Delta c_{ij} \cos \Delta a_{ij})$  (i.e. cosine error), where  $\Delta L_{ij}^*$  represents the distance from the spindle's nominal reference point,  $p_i^*$ , to the retroreflector's position,  $P_j^*$ .  $u_4$  is calculated from  $u_{41}$  and  $u_{42}$  by using the Monte Carlo simulation applied to this relationship.

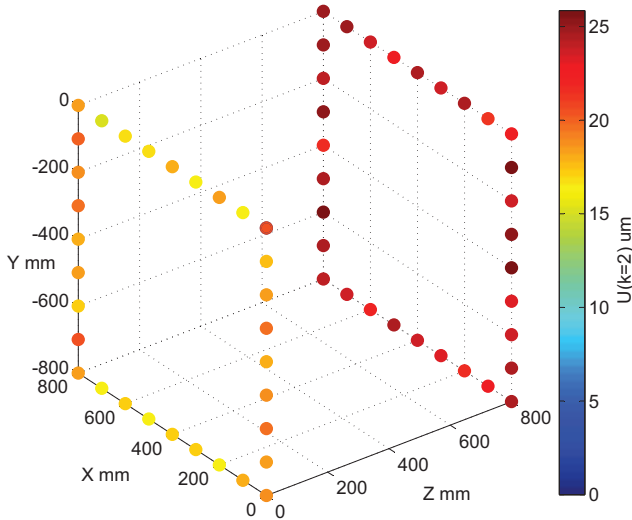


Fig. 13. Assessed uncertainty in estimated target positions propagated from the uncertainty in laser displacements shown in Tabel V. The color represents the extended uncertainty ( $k = 2$ ) of the distance of the estimated target position to its command position.

Radial error motions of rotary axes also directly influence the measurement uncertainty. The uncertainty analysis showed that the laser beam's direction error, caused by the "open-loop" regulation, does not impose significant contribution on the

measurement uncertainty, when the machine tool has practical "normal" accuracy. The experiment showed the performance of the proposed scheme to estimate the machine's 3D positions over  $800 \times 800 \times 800$  mm workspace.

## REFERENCES

- [1] ISO 230-1:2012, Test code for machine tools – Part 1: Geometric accuracy of machines operating under no-load or quasi-static conditions.
- [2] ISO/TR 16907:2015, Numerical compensation of geometric errors of machine tools.
- [3] S. Ibaraki, W. Knapp, Indirect measurement of volumetric accuracy for three-axis and five-axis machine tools: a review. *Int. J. Autom. Technol.* 6(2) (2012) 110-124.
- [4] H. Schwenke, W. Knapp, H. Haitjema, A. Weckenmann, R. Schmitt, F. Delbressine, Geometric error measurement and compensation of machines –An update, *Ann. CIRP – Manuf. Technol.*, 57(2) (2008) 560-575.
- [5] K. Lau, R. Hocken, W. Haight, Automatic laser tracking interferometer system for robot metrology, *Precis. Eng.* 8(1) (1986) 3-8.
- [6] B. Muralikrishnan, S. Phillips, and D. Sawyer, Laser trackers for large-scale dimensional metrology: A review, *Precis. Eng.* 44 (2016) 13-28.
- [7] G.N. Peggs, Virtual technologies for advanced manufacturing and metrology, *Int'l J. of Computer Integrated Manufacturing*, 16(7/8) (2003).
- [8] E.B. Hughes, A. Wilson, G.N. Peggs, Design of a high-accuracy CMM based on multi-lateration techniques, *Ann. CIRP – Manuf. Technol.* 49(1) (2000) 391-394.
- [9] S. Ibaraki, T. Kudo, T. Yano, T. Takatsuji, S. Osawa, O. Sato, Estimation of three-dimensional volumetric errors of machining centers by a tracking interferometer, *Precis. Eng.* 39 (2014) 179-186.
- [10] H. Schwenke, M. Franke, J. Hannaford, H. Kunzmann, Error mapping of CMMs and machine tools by a single tracking interferometer, *Ann. CIRP – Manuf. Technol.*, 54(1) (2005) 475-478.

- [11] H. Schwenke, R. Schmitt, P. Jatzkowski, C. Warmann, On-the-fly calibration of linear and rotary axes of machine tools and CMMs using a tracking interferometer, *Ann. CIRP – Manuf. Technol.*, 58(1) (2009) 477-480.
- [12] S. Ibaraki, G. Sato, K. Takeuchi, ‘ Open-loop ’ tracking interferometer for machine tool volumetric error measurement – Two-dimensional case, *Precis. Eng.* 38(3) (2014) 666-672.
- [13] S. Ibaraki, K. Nagae, G. Sato, Proposal of ‘ ‘ open-loop ’ ’ tracking interferometer for machine tool volumetric error measurement, *Ann. CIRP – Manuf. Technol.* 63(1) (2014) 501-504.
- [14] ISO 10791-1:2015, Test conditions for machining centres – Part 1: Geometric tests for machines with horizontal spindle (horizontal Z-axis).
- [15] T. Takatsuji, M. Goto, S. Osawa, R. Yin, T. Kurosawa, Whole-viewing-angle cat’s-eye retroreflector as a target of laser trackers, *Measurement Science and Technology*, 10(7) (1999) 87-90.
- [16] Huo D, Maropoulos PD, Cheng CH, The Framework of the Virtual Laser Tracker – A Systematic Approach to the Assessment of Error sources and Uncertainty in Laser Tracker Measurement, *Proc. the 6th CIRP-Sponsored Int. Conf. on Digital Enterprise Technology*, (2010) 507-523
- [17] Teoh PL, Shirinzadeh B, Foong CW, Alici G, The measurement uncertainties in the laser interferometry-based sensing and tracking technique, *Measurement*, 32(2) (2002) 135-150
- [18] JCGM 100:2008, Evaluation of measurement data - Guide to the expression of uncertainty in measurement (GUM), 2008.
- [19] Bringmann B, Besuchet J, Rohr L, Systematic evaluation of calibration methods, *CIRP Annals Manuf. Tech.*, 57(1) (2008) 529-532.